The Cryosphere Discuss., 6, 505–530, 2012
www.the-cryosphere-discuss.net/6/505/2012/
doi:10.5194/tcd-6-505-2012

The Cryosphere Discussions

Quantification of ikaite in Antarctic sea ice

M. Fischer[1,6], D. N. Thomas[2,3], A. Krell[1], G. Nehrke[1], J. Göttlicher[4], L. Norman[2], C. Riaux-Gobin[5], and G. S. Dieckmann[1]

[1]Alfred Wegener Institute for Polar and Marine Reserach, Bremerhaven, Germany
[2]Ocean Sciences, College of Natural Sciences, Bangor University, Menai Bridge, UK
[3]Marine Centre, Finnish Environment Institute (SYKE), Helsinki, Finland
[4]Institute of Synchrotron Radiation (ISS), Synchrotron Radiation Source ANKA, Karlsruhe Institute of Technology, Eggenstein-Leopoldshafen, Germany
[5]USR3278, CRIOBE, CNRS-EPHE, Perpignan, France
[6]Faculty of Biology and Chemistry, University of Bremen, Bremen, Germany

Received: 18 January 2012 – Accepted: 25 January 2012 – Published: 3 February 2012

Correspondence to: M. Fischer (michael.fischer@awi.de)

Published by Copernicus Publications on behalf of the European Geosciences Union.

Abstract

Calcium carbonate precipitation in sea ice can increase pCO_2 during precipitation in winter and decrease pCO_2 during dissolution in spring. $CaCO_3$ precipitation in sea ice is thought to potentially drive significant CO_2 uptake by the ocean. However, little is known about the quantitative spatial and temporal distribution of $CaCO_3$ within sea ice. This is the first quantitative study of hydrous calcium carbonate, as ikaite, in sea ice and discusses its potential significance for the carbon cycle in polar oceans. Ice cores and brine samples were collected from pack and land fast sea ice between September and December 2007 during an expedition in the East Antarctic and another off Terre Adélie, Antarctica. Samples were analysed for $CaCO_3$, Salinity, DOC, DON, Phosphate, and total alkalinity. A relationship between the measured parameters and $CaCO_3$ precipitation could not be observed. We found calcium carbonate, as ikaite, mostly in the top layer of sea ice with values up to 126 mg ikaite per liter melted sea ice. This potentially represents a contribution between 0.12 and 9 Tg C to the annual carbon flux in polar oceans. The horizontal distribution of ikaite in sea ice was heterogenous. We also found the precipitate in the snow on top of the sea ice.

1 Introduction

Sea ice covers up to 7 % of the total surface area of the oceans at its maximum extent (Comiso, 2010). The physical barrier itself has a major impact on the gas exchange between atmosphere and ocean, and recently the discussion has extended to considering how physical and biogeochemical processes within the ice itself can affect diffusion and flux of gases to both atmosphere and ocean (Tison et al., 2002; Delille, 2006; Rysgaard et al., 2007, 2009, 2011; Miller et al., 2011; Loose et al., 2011). On the basis of thermodynamic equilibrium calculations, the precipitation of $CaCO_3$ was predicted to occur in natural sea ice formation (Gitterman, 1937; Jones and Coote, 1981; Anderson and Jones, 1985) and it was proposed to precipitate as calcite (Marion, 2001). However,

actual evidence was, for a long time, only indirect (Killawee et al., 1998; Papadimitriou et al., 2004; Tison et al., 2002) until Dieckmann et al. (2008) found calcium carbonate as ikaite $CaCO_3 \cdot 6H_2O$ in Antarctic sea ice, and more recently in Arctic sea ice (Dieckmann et al., 2010). Rysgaard et al. (2007, 2009) showed that with brine, dissolved organic carbon (DIC) is rejected from growing sea ice to the underlying waters. They ascribe the high pCO_2 levels found below sea ice to calcium carbonate precipitation. Delille et al. (2007) also claim that $CaCO_3$ precipitation in sea ice could drive significant CO_2 uptake by the ocean and therefore contribute significantly to a polar carbon pump.

Besides its function as a component in the carbon cycle, the mineral is also thought to have a key role in tropospheric ozone depletion events (ODEs) at high latitudes (Sander et al., 2006; Sander and Morin, 2010). Simulations of the chemistry occurring in polar regions over recently formed sea ice relate the ODE to the transformation of inert sea-salt bromide to reactive bromine monoxide (BrO) when precipitation of calcium carbonate from freezing sea water is taken into account. The discovery of ikaite in firn ice of the Antarctic continent, which appears to be derived from sea ice 300 km away, may also have implications for its use as a sea ice proxy (Sala et al., 2008). However, to date most studies of calcium carbonate in sea ice have been mainly qualitative and little is known about the spatial and temporal distribution of $CaCO_3$ within sea ice. There is also a lack of knowledge on the exact conditions leading to ikaite precipitation as well as on the amount and fate of ikaite: e.g. one assumption is that phosphate and dissolved organic matter (DOM) may reduce the precipitation of calcium carbonate (Bischoff et al., 1993; Zullig and Morse, 1988).

The objective of this study therefore was to: (1) Provide the first systematic observation and quantification of $CaCO_3$ precipitation in Antarctic sea ice on a spatial and temporal scale and (2) to investigate relationships between calcium carbonate and alkalinity, phosphate, and dissolved organic matter.

2 Methods

Two campaigns were performed between September and December 2007. During the first campaign (Sea Ice Physics and Ecosystem eXperiment (SIPEX) onboard RSV Aurora Australis) fourteen ice cores (S1 to S14) were taken at different locations between 64° and 66° south and 116° and 128° east (Fig. 1). The cores were cut into 10 cm sections within a few minutes after sampling and stored in plastic containers. Ice cores from station S1 to S4 and S6 to S14 represent pack ice with different degrees of deformation (Table 1). The ice core from station S5 was taken from fast ice between grounded icebergs. Further details on ice types, see Table 1, van der Merwe et al. (2009) and Meiners et al. (2011). A general description of the ice conditions during the expedition can be found in Worby et al. (2011). Brine from sackholes from 10 out of 14 stations (see Table 2) was collected for nutrient and DOM analyses (see Norman et al., 2011).

On the second campaign (from November to December 2007) sea ice samples were collected close to the French base Dumont d'Urville, 66° 39′13″ S 140°00′5″ E near station C described in Delille et al. (2007). Six complete ice cores (D1 to D6) were taken from young fast sea ice (age: ≈ 3 month, Anne Jacquet, personal communication) which had formed in August. This area was predominantly free of snow with only isolated patches of snow being present. The cores were also cut into 10 cm sections and stored as described above. In order to determine small-scale vertical distribution of ikaite, we also collected four surface cores (D7 to D10) between 10 and 15 cm length (Table 1). Cores D7 and D9 were taken from the main sampling site without any snow on top, while D8 was taken next to it and included snow. Ice sample D10 was taken from older fast ice approximately 200 m away from the main sampling site. This core was taken from sea ice which had formed in autumn and had remained intact since its formation, in contrast to cores D1–D9 which were from younger sea ice. These cores were cut into 2 cm sections. In addition, to determine horizontal spatial variability of calcium carbonate, we chose an area 50 m away from the first sampling site. On this

site the first top 10 cm of fast ice were sampled every 5 m (x and y direction) in a grid of 20 m by 20 m (D-SP1 to D-SP25, Table 1). The partial ice cores obtained were stored in clean plastic containers. At the main sampling site, sackholes (D-SH1 to D-SH7) of 30 cm were cored every two or three days for a temporal analysis of brine and ice from an area of 10 m × 10 m to minimize bias from spatial heterogeneity. The partial ice core obtained from these sackholes was also stored in clean plastic containers. Brine was allowed to collect in the sackholes and sampled with a vacuum pump and transferred into different vials for total alkalinity (TA), dissolved organic carnon (DOC), dissolved organic nitrogen (DON), and phosphate analyses. Samples for DOM and nutrients were filtered through 0.2 µm cellulose acetate filter and kept frozen until analyses within 6 months. The TA samples were measured directly in the base laboratory.

We also sampled glacial firn ice 6 km away from the ice shelf at Prud'homme to test if calcium carbonates are found on the ice shelf in this region. One surface core (1 m) was collected and cut into 3 equal sections. The sections were stored in plastic containers and brought to the base laboratory.

All sea ice samples were slowly melted in a climate controlled room where the temperatures never exceeded 4 °C to avoid decomposition of the mineral ikaite. Regular monitoring (several times a day) guaranteed a processing of the samples as soon as the cores, or sections were melted. This ensured that the temperature of the melt water never rose above 0 °C. The melt water was filtered through 0.2 µm polycarbonate filters and the volume determined. The filters with crystals were then placed in a plastic vial containing 75 % ethanol and frozen at −18 °C for later mineralogical phase identification and quantitative measurements. In several instances crystals were collected after swirling the melted samples and allowing crystals to settle in the resulting vortex. The crystals were transferred from the vortex to a petri dish using a glass pipette (see Dieckmann et al., 2008, for methods). These were briefly inspected under the binocular microscope and photographed to check the morphology and subsequently also filtered as described above.

Mineral phase identification was conducted by micro X-ray diffraction (µ-XRD) under cryogenic conditions on selected samples at the Synchrotron Laboratory for Environmental Studies SUL-X at the synchrotron radiation source ANKA, Forschungszentrum Karlsruhe (now Kalsruhe Institute of Technology) as described by Dieckmann et al. (2008).

To quantify the amount of ikaite within the sample, the quantity of calcium ions were determined using Inductively-Coupled Plasma Optical Emission Spectrometry (ICP OES). The plastic caps containing the filter were rinsed with concentrated ethanol and the content was transferred to larger vials. The transferred samples were dried at 60 °C until all the ethanol had evaporated. Five ml concentrated HNO_3 was added to dissociate all molecules before the samples were analysed in the ICP OES. The amount of ikaite was calculated based on the measured calcium.

Brines from sackholes (D-SH1 to D-SH7 and from 10 stations during the SIPEX campaign) were analyzed for in situ concentrations of phosphate, dissolved organic nitrogen (DON), dissolved organic carbon (DOC) and alkalinity (Table 2). Analysis for the major dissolved inorganic nutrients, nitrate (NO_3^-), nitrite (NO_2^-) and of dissolved inorganic phosphorus (DIP) was done using standard colorimetric methodology (Hanson and Koroleff, 1983) as adapted for flow injection analysis (FIA) on a LACHAT Instruments Quick-Chem 8000 autoanalyzer (Hales et al., 2004). Dissolved organic carbon was analysed by high temperature combustion on an MQ1000 TOC analyzer according to Qian and Mopper (1996). Dissolved organic nitrogen was determined by subtraction of NO_3^-, and NH_4^+ from the total dissolved nitrogen (TDN) analyzed using on-line peroxodisulfate oxidation coupled with ultraviolet radiation at pH 9.0 and 100 °C (Kroon, 1993). Total alkalinity (D-SH1 to D-SH7) was measured at the station laboratory within one day after sampling as described by Nomura et al. (2010).

For the spatial analyses of the horizontal distribution of $CaCO_3 \cdot 6H_2O$ a conventional geostatistical spatial interpolation was applied by using the simple kriging method (Sarma, 2009).

3 Results

Calcium carbonate crystals were found in all samples analyzed, including snow, sea ice and glacial ice. Mineral phase identification of selected samples confirmed that ikaite was the precipitate present. Since all crystals extracted from the ice cores showed the same morphological features, it is most likely that the XRD identification as ikaite is representative for all crystals found in this study (Fig. 2). Ikaite concentrations ranged from 0.01 to 126 mg l^{-1} melted sea ice. The maximum amount of ikaite was found in older fast ice. Data from 14 ice cores of the SIPEX campaign show clearly the distribution of the ikaite crystals with highest concentrations in the top layers of ice (Fig. 3). Though the highest value in pack ice was 9.5 mg ikaite l^{-1} melted sea ice, most of the values in the first ten centimeters did not exceed 2 mg ikaite l^{-1}. Below a depth of 20 cm (with the exception of two ice cores, S3 and S6) in the pack ice, ikaite concentrations ranged between 0.02 and 0.3 mg l^{-1}. Ice texture analyses of cores S3 and S6 showed it to be rafted sea ice.

The ikaite concentrations in land fast ice off Terre Adélie were of a similar magnitude but generally higher than the pack ice cores (Fig. 4): Most were between 2 and 5 mg l^{-1} in the top layer. A higher resolution sampling (2 cm) over the first 10 to 15 cm showed that the highest concentrations of the mineral were in the top 2 to 4 cm of the cores (Fig. 5). Ice core D10 (Fig. 6) was taken at a location of older fast ice 133 cm thick, 200 m away from the initial sampling site. This core had higher mineral concentrations than those from the younger sea ice. Ice core D8 from snow covered ice (Fig. 7) had ikaite crystals throughout the core and even in the snow itself. The highest concentration (38.77 mg l^{-1} melted sea ice) was observed at the snow/ice interface. Salinity profiles were similar to those of the amount of ikaite in core D8 (Fig. 7).

A temporal change in ikaite concentration during the period of sampling between 14 to 27 November 2007 was not observed. Values of the temporal and spatial experiment are in the same range (0.06 to 3.93 mg l^{-1}, Fig. 8, Table 2). Hence, we could not differ temporal from spatial heterogeneity. Values from the spatial experiment showed that the distribution of $CaCO_3 \cdot 6H_2O$ in sea ice is already heterogenous.

Normalized to a salinity of 35, (see Papadimitriou et al., 2009) dissolved organic nitrogen (DON_{35}) and dissolved organic carbon (DOC_{35}) concentrations in the brines increased, non-linearly, over the study time. Although phosphate (normalized to $S = 35$) shows the same trend as DON_{35} and DOC_{35} at the beginning, it did not increase over time and remained low. Only NO_3 shows a trend which might indicate biological activity. Alkalinity fell from almost 2600 to approximately 2200 µmol l^{-1}. TA did not show a linear trend, similar to the other measured chemical parameters. Neither phosphate, DON, DOC concentrations (from SIPEX and DDU campaign) nor TA (DDU campaign) correlated significantly with the amount of hydrous calcium carbonate present in the ice horizons from where the brines were collected from.

4 Discussion

Our results together with previous observations (Dieckmann et al., 2008) indicate, that calcium carbonate precipitation is widespread in Antarctic sea ice, albeit that its concentration is heterogenous, as is the case for most other biogeochemical parameters in sea ice (Thomas and Dieckmann, 2010). Although we were not able to verify the $CaCO_3$ polymorph for each sample collected, the visual characterisation by light microscopy confirmed that the morphology of all crystals was identical to those analyzed by X-ray diffraction. We are therefore convinced that ikaite was always the precipitate. Higher brine salinities, and correspondingly high Ω_{ikaite} (ikaite saturation state of seawater) values, resulted in a more likely precipitation of ikaite near the surface than in lower parts in sea ice where temperatures are higher and brine salinity can drop to seawater values. However, it is still not clear at what point in time ikaite precipitation occurs, and our interpretation is confounded because the various biogeochemical parameters measured during sample collection do not reflect conditions at the time of precipitation.

Based on a thermomolecular pressure gradient as described by Wettlaufer and Worster (1995), brine, as unfrozen liquid, is transported from the ice interior toward

the relatively colder surface (Rankin and Wolff, 2002). The accumulated brine at the surface has a salinity of about 100 (Perovich and Richter-Menge, 1994) and favors the precipitation of salts. Under those conditions frost flowers may start to grow (Perovich and Richter-Menge, 1994; Rankin and Wolff, 2002; Obbard et al., 2009). However, conditions not necessarily leading to frost flower formation, may also lead to $CaCO_3$ precipitation if the temperature is low and salinity is high. It appears that hydrous calcium carbonate precipitation also takes place during subsequent sea ice growth as observed in older land fast ice (Fig. 6). The occurrence of calcium carbonate in the snow cover can also be explained by the thermomolecular pressure gradient and capillary transport, which is supported by the maximum occurrence of ikaite at the snow ice interface as described above (Fig. 7).

Higher values of calcium carbonate in some middle layers of sea ice were attributable to rafting of floes subsequent to sea ice formation. Floes which slide over each other where the surface layer of one of the floes is transformed into a middle layer of the resulting one. Although $CaCO_3$ concentrations were on the same order of magnitude in pack ice and land fast ice there appear to be differences in the amount of precipitated calcium carbonate. The highest values were recorded in approximately 1 yr old land fast sea ice, followed by high amounts in land fast ice and the lowest in pack ice.

It is not possible to determine the temporal development of $CaCO_3$ in the sea ice investigated. This is due to the extreme variability in $CaCO_3$ concentration even on small scales. The reason for this heterogeneity might be due to the inherent variability in many sea ice properties ranging from temperature, salinity, texture, chemistry and lastly bacterial activity. The spatial and temporal heterogeneity are already apparent on small scales as shown by the spatial and temporal studies. Analyses, however, show a similar range in the data for both campaigns. Thus, it is difficult to draw conclusions on the temporal evolution of the precipitation of ikaite.

The high concentrations of DOC and DON found in sea ice during the campaign off Terre Adélie were expected to inhibit $CaCO_3$ precipitation (Bischoff et al., 1993). Zullig and Morse (1988) and Berner et al. (1978) have shown that DOM influences the

precipitation of calcium carbonate. However, these studies refer only to the inhibition for anhydrous polymorphs of $CaCO_3$. Besides the repression by polyphosphate and magnesium ions on the precipitation of anhydrous calcium carbonate in favour of hydrated forms, Dickens and Brown (1970) postulate that hydrated salts may play an important part in biological mineralization. Taking this into account, additionally to the elevated Ω_{ikaite}, microbial biomass, such as cell surfaces and/or EPS, catalyze the precipitation of calcium carbonate (Kandianis et al., 2008). This also coincides with findings of elevated abundance of bacteria and exopolymers in frost flowers (Bowman and Deming, 2010) and the top layer of sea ice (Aslam et al., 2012) which supports the hypothesis of $CaCO_3$ precipitation during frost flowers and sea ice formation as discussed above.

Previous studies have pointed out the importance of sea ice for the carbon uptake in polar oceans due to i.e. $CaCO_3$ precipitation (Rysgaard et al., 2009, 2011; Delille, 2006; Tison et al., 2002; Nedashkovsky et al., 2009). Based on our observations we propose a first estimate of the possible contribution of calcium carbonate precipitation to the carbon cycle. For simplicity we take into account only the top 10 cm of sea ice, since the amount in the lower part was negligible. Absolute values of ikaite found in the top 10 cm of sea ice ranged between 0.1 and 6.5 $g\,m^{-2}$. Based on the total seasonal ice cover in the Antarctic (Comiso, 2010) we calculate that $CaCO_3$ formation in sea ice potentially could represent a contribution of between 0.1 and 6 Tg C to the carbon flux in the Southern Ocean. Assuming the same distribution in Arctic sea ice together with the ice cover from Comiso and Nishio (2008) then the precipitation of $CaCO_3$ would be responsible for a flux between 0.04 and 3 TgC. For both the Arctic and Antarctic this would be between 0.1 % and 4.5 % of the air-sea CO_2 flux in open oceanic water at high latitudes (Takahashi et al., 2009; Rysgaard et al., 2011) or up to 13 % for the Southern Ocean south of 50° (Takahashi et al., 2009). Though there is a large amount of ikaite in the snow, the amount of $CaCO_3$ therein was not taken into account for the calculation, since the distribution of $CaCO_3$ crystals in the snow remains elusive. However, of widespread this would be a significant addition to the polar carbon flux. Considering polynyas with new sea ice forming during the winter and

taking into account, that $CaCO_3$ precipitation mainly occurs during young sea ice and frost flower formation, this phenomenon might then contribute even to a larger extent to the air-sea flux. However, this would be only the case if CO_2, which is released during $CaCO_3$ precipitation, is rejected to the underlying water column. While sea ice is still permeable during sea ice formation, high pCO_2 in brine, and $CaCO_3$ precipitation in the top layer of sea ice, a large amount of CO_2 would be released to the atmosphere and would thus not contribute to the sea ice carbon pump as proposed by Rysgaard et al. (2007, 2011) and Loose et al. (2011). It would be essential to determine and quantify the CO_2 pathways during sea ice formation to fully quantify the contribution of calcium carbonate precipitation to the air-sea CO_2 flux.

With ikaite mainly in the top layer of sea ice our findings support the work of Sander et al. (2006) and Sander and Morin (2010) which describes the contribution of $CaCO_3$ precipitation to ozone depletion events. It also supports the work of Sala et al. (2008), since ikaite crystals at the snow-ice interface and in the snow are more likely exposed to aeolian transport.

5 Conclusions

This is the first study providing a systematic investigation of the spatial and temporal distribution of $CaCO_3$ in sea ice. We showed the heterogenous occurrence of $CaCO_3$ in sea ice and provide an estimate of its significance for the carbon cycle in polar oceans. However, larger scale quantification of $CaCO_3$ precipitation in different types of sea ice in both the Arctic and Antarctic is necessary to validate these findings. Since parameters measured during sample collection do not reflect conditions at the time of precipitation, much work is needed to evaluate the conditions of calcium carbonate precipitation within sea ice and its fate during sea ice melt.

Acknowledgements. We thank the EPONTA (EPONTic micro-algae adapted to sea-ice) program for funding and Institut Polaire Français, Paul-Émile Victor (IPEV) for the logistic assistance during the DDU campaign. We thank Harald Zöller, Thomas Spangenberg, Michael Wünsch, and Karlheinze Cerff (all at Forschungszentrum Karslruhe) for technical and computing support before and during the measurements, as well as Christiane Uhlig for preparing the samples for mineralogy and synthetic ikaite and photography. We also thank Frank Gérard, all the scientists, and technicians from the french research station Dumont d'Urville, Antarctica as well as the captain and crew of the polar vessel Astrolabe and the pilots of the Australian Antarctic Division for all their help and support. David Thomas and Louiza Norman thank NERC (UK) and the Leverhulme Trust for funding. We thank the DFG for financial support through grand NE 1564/2-1 (SPP1158).

References

Anderson, L. G. and Jones, E. P.: Measurement of total alkalinity, calcium, and sulfate in natural sea ice, J. Geophys. Res., 90, 9194–9198, 1985. 506

Aslam, S., Underwood, G. J. C., Kaartokallio, H., Norman, L., Autio, R., Fischer, M., Kuosa, H., Dieckmann, G. S., and Thomas, D.: Dissolved extracellular polymeric substance (dEPS) dynamics and bacterial growth during sea ice formation in an ice tank study, Polar Biol., doi:10.1007/s00300-011-1112-0, in press, 2012. 514

Berner, R., Westrich, J. T., Graber, R., Smitz, J., and Martens, C.: Inhibition of aragonite precipitation from supersaturated seawater, Am. J. Sci., 278, 816–837, 1978. 513

Bischoff, J. L., Fitzpatrick, J. A., and Rosenbauer, R. J.: The solubility and stabilization of ikaite $CaCO_3 \cdot H_2O$ from 0° to 25 °C: environmental and paleoclimatic implications for Thinolite Tufa, J. Geol., 101, 21–33, 1993. 507, 513

Bowman, J. and Deming, J.: Elevated bacterial abundance and exopolymers in saline frost flowers and implications for atmospheric chemistry and microbial dispersal, Geophys. Res. Lett., 37, L13501, doi:10.1029/2010GL043020, 2010. 514

Comiso, J. C.: Large-scale characteristics and variability of the global sea ice cover, in: Sea Ice: An Introduction to its Physics, Chemistry, Biology and Geology, edited by: Thomas, D. N. and Dieckmann, G. S., Blackwell, Oxford, 2010. 506, 514

Comiso, J. C. and Nishio, F.: Trends in the sea ice cover using enhanced and compatible AMSR-E, SSM/I, and SMMR data, J. Geophys. Res, 113, C02S07, doi:10.1029/2007JC004257, 2008. 514

Delille, B.: Inorganic carbon dynamics and air-ice-sea CO_2 fluxes in the open and coastal waters of the Southern Ocean, Ph. D. thesis, Université de Liège, Liège, 2006. 506, 514

Delille, B., Jourdain, B., Borges, A. V., Tison, J.-L., and Delille, D.: Biogas CO_2, O_2, dimethylsulfide) dynamics in spring Antarctic fast ice, Limnol. Oceanogr, 52, 1367–1379, 2007. 507, 508

Dickens, B. and Brown, W. B.: The crystal structure of calcium carbonate hexahydrate at ∼ −120°, Inorgan. Chem., 9, 480–486, 1970. 514

Dieckmann, G. S., Nehrke, G., Papadimitriou, S., Göttlicher, J., Steininger, R., Kennedy, H., Wolf-Gladrow, D., and Thomas, D. N.: Calcium carbonate as ikaite crystals in Antarctic sea ice, Geophys. Res. Lett., 35, L08 501, doi:10.1029/2008GL033540, 2008. 507, 509, 510, 512

Dieckmann, G. S., Nehrke, G., Uhlig, C., Göttlicher, J., Gerland, S., Granskog, M. A., and Thomas, D. N.: Brief Communication: Ikaite ($CaCO_3 \cdot 6H_2O$) discovered in Arctic sea ice, The Cryosphere, 4, 227–230, doi:10.5194/tc-4-227-2010, 2010. 507

Gitterman, K. E.: Thermal analysis of seawater, CRRELTL287, USACRREL, Hanover, New Hampshire, 1937. 506

Hanson, H. and Koroleff, F.: Determination of nutrients, in: Methods of Seawater Analysis, edited by: Grasshoff, K., Ehrhardt, M., and Kremling, K., Wiley-VCH, Weinheim, 159–228, 1983. 510

Jones, E. P. and Coote, A. R.: Oceanic CO_2 produced by the precipitation of $CaCO_3$ from brines in sea ice, J. Geophys. Res., 86, 11041–11043, 1981. 506

Kandianis, M., Fouke, B., Johnson, J., and Inskeep, W.: Microbial biomass: a catalyst for $CaCO_3$ precipitation in advection-dominated transport regimes, Geol. Soc. Am. B., 120, 442–450, 2008. 514

Killawee, J. A., Fairchild, I. J., Tison, J.-L., Janssens, L., and Lorrain, R.: Segregation of solutes and gases in experimental freezing of dilute solutions: implications for natural glacial systems, Geochim. Cosmochim. Ac., 62, 3637–3655, 1998. 507

Kroon, H.: Determination of nitrogen in water: comparison of continuous flow method with online UV digestion with the original Kjedahl method, Anal. Chim. Acta, 276, 287–293, 1993. 510

Loose, B., Miller, L., Elliott, S., and Papakyriakou, T.: Sea ice biogeochemistry and material transport across the frozen interface, Oceanography, 24(3), 202–218, doi:10.5670/oceanog.2011.72, 2011. 506, 515

Marion, G. M.: Carbonate mineral solubility at low temperatures in the Na-K-Mg-Ca-H-Cl-SO_4-OH-HCO_3-CO_3-CO_2-H_2O system, Geochim. Cosmochim. Ac., 65, 1883–1896, 2001. 506

Meiners, K., Norman, L., Granskog, M. A., Krell, A., Heil, P., and Thomas, D. N.: Physico-ecobiogeochemistry of East Antarctic pack ice during the winter-spring transition, Deep-Sea Res. Pt. II, 58, 1172–1181, doi:10.1016/j.dsr2.2010.10.033, 2011. 508

Miller, L., Papakyriakou, T., Collins, E., Deming, J., Ehn, J., Macdonald, R., Mucci, A., Owens, O., Raudsepp, M., and Sutherland, N.: Carbon dynamics in sea ice: a winter flux time series, J. Geophys. Res., 116, C02028, doi:10.1029/2009JC006058, 2011. 506

Nedashkovsky, A., Khvedynich, S., and Petrovsky, T.: Alkalinity of sea ice in the high-latitudinal arctic according to the surveys performed at north pole drifting station 34 and characterization of the role of the arctic ice in the CO_2 exchange, Mar. Chem., 49, 61–69, 2009. 514

Nomura, D., Yoshikawa-Inoue, H., Toyota, T., and Shirasawa, K.: Effects of snow, snowmelting and refreezing processes on air–sea-ice CO_2 flux, J. Glaciol., 56, 262–270, 2010. 510

Norman, L., Thomas, D. N., Stedmon, C. A., Granskog, M. A., Papadimitriou, S., Krapp, R. H., Meiners, K. M., Lannuzel, D., van der Merwe, P., and Dieckmann, G. S.: The characteristics of dissolved organic matter (DOM) and chromophoric dissolved organic matter (CDOM) in Antarctic sea ice, Deep-Sea Res. Pt. II, 58, 1075–1091, doi:10.1016/j.dsr2.2010.10.030, 2011. 508

Obbard, R. W., Roscoe, H. K., Wolff, E. W., and Atkinson, H. M.: Frost flower surface area and chemistry as a function of salinity and temperature, J. Geophys. Res., 114, D20305, doi:10.1029/2009JD012481, 2009. 513

Papadimitriou, S., Kennedy, H., Kattner, G., Dieckmann, G. S., and Thomas, D. N.: Experimental evidence for carbonate precipitation and CO_2 degassing during sea ice formation, Geochim. Cosmochim. Ac., 68, 1749–1761, doi:10.1016/j.gca.2003.07.004, 2004. 507

Papadimitriou, S., Thomas, D., Kennedy, H., Kuosa, H., and Dieckmann, G. S.: Inorganic carbon removal and isotopic enrichment in Antarctic sea ice gap layers during early austral summer, Mar. Ecol. Progr. Ser., 386, 15–27, 2009. 512

Perovich, D. K. and Richter-Menge, J. A.: Surface characteristics of lead ice, J. Geophys. Res., 99, 16341–16350, 1994. 513

Qian, J. and Mopper, K.: An automated, high performance, high temperature combustion dissolved organic carbon analyzer, Anal. Chem., 68, 3090–3097, 1996. 510

Rankin, A. M. and Wolff, E. W.: Frost flowers: implications for tropospheric chemistry and ice core interpretation, J. Geophys. Res., 107, 4683, doi:10.1029/2002JD002492, 2002. 513

Rysgaard, S., Glud, R. N., Sejr, M. K., Bendtsen, J., and Christensen, P. B.: Inorganic carbon transport during sea ice growth and decay: a carbon pump in polar seas, J. Geophys. Res., 112, C03 016, doi:10.1029/2006JC003572, 2007. 506, 507, 515

Rysgaard, S., Bendtsen, J., Pedersen, L. T., Ramløv, H., and Glud, R. N.: Increased CO_2 uptake due to sea ice growth and decay in the Nordic Seas, J. Geophys. Res., 114, C09011, doi:10.1029/2008JC005088, 2009. 506, 507, 514

Rysgaard, S., Bendtsen, J., Delille, B., Dieckmann, G. S., Glud, R. N., Kennedy, H., Mortensen, J., Papadimitriou, S., Thomas, D. N., and Tison, J. L.: Sea ice contribution to the air-sea CO_2 exchange in the Arctic and Southern Oceans, Tellus B, 63, 823–830, 2011. 506, 514, 515

Sala, M., Delmonte, B., Frezzotti, M., Proposito, M., Scarchilli, C., Maggi, V., Artioli, G., M, D., Marino, F., Ricci, P., and De Giudici, G.: Evidence of calcium carbonates in coastal (Talos Dome and Ross Sea area) East Antarctica snow and firn: environmental and climatic implications, Earth Planet. Sci. Lett., 271, 43–52, doi:10.1016/j.epsl.2008.03.045, 2008. 507, 515

Sander, R. and Morin, S.: Introducing the bromide/alkalinity ratio for a follow-up discussion on "Precipitation of salts in freezing seawater and ozone depletion events: a status report", by Morin et al., published in Atmos. Chem. Phys., 8, 7317–7324, 2008, Atmos. Chem. Phys., 10, 7655–7658, doi:10.5194/acp-10-7655-2010, 2010. 507, 515

Sander, R., Burrows, J., and Kaleschke, L.: Carbonate precipitation in brine – a potential trigger for tropospheric ozone depletion events, Atmos. Chem. Phys., 6, 4653–4658, doi:10.5194/acp-6-4653-2006, 2006. 507, 515

Sarma, D.: Geostatistics with Applications in Earth Sciences, 2nd edn., Springer, Heidelberg, 2009. 510

Takahashi, T., Sutherland, S., Wanninkhof, R., Sweeney, C., Feely, R., Chipman, D. W., Hales, B., Friederich, G., Chavez, F., Sabine, C., Watson, A., Bakker, D., Schuster, U., Metzl, N., Yoshikawa-Inoue, H., Ishii, M., Midorikawa, T., Nojiri, Y., Körtzinger, A., Steinhoffm, T., Hoppema, M., Olafsson, J., Arnarson, T., Tilbrook, B., Johannessen, T., Olsen, A., Bellerby, R., Wong, C., Delille, B., Bates, N., and de Baar, H.: Climatological mean and decadal change in surface ocean pCO_2, and net sea–air CO_2 flux over the global oceans, Deep-Sea Res., 56, 554–577, doi:10.1016/j.dsr2.2008.12.009, 2009. 514

Thomas, D. N. and Dieckmann, G. S.: Sea Ice, 2nd edn., Wiley-Blackwell Publishing, Oxford, 2010. 512

Tison, J. L., Haas, C., Gowing, M. M., Sleewaegen, S., and Bernard, A.: Tank study of physico-chemical controls on gas content and composition during growth of young sea ice, J. Glaciol., 48, 177–191, 2002. 506, 507, 514

van der Merwe, Lannuzel, D., Mancuso Nichols, C., Meiners, K., Heil, P., Norman, L., Thomas, D., and Bowie, A.: Biogeochemical observations during the winter–spring transition in East Antarctic sea ice: evidence of iron and exopolysaccharide controls, Mar. Chem., 115, 163–175, 2009. 508

Wettlaufer, J. S. and Worster, M. G.: Dynamics of premelted films: frost heave in a capillary, Phys. Rev. E, 51, 4679–4689, 1995. 512

Zullig, J. J. and Morse, J. W.: Interaction of organic acids with carbonate mineral surfaces in seawater and related solutions: I. Fatty acid adsorption, Geochim. Cosmochim. Ac., 52, 1667–1678, 1988. 507, 513

Table 1. Types and thickness of sea ice during SIPEX and DDU campaign.

Sample	Cruise	Sample type	Sample thickness in cm
S1	SIPEX	Pack ice	51
S2	SIPEX	Pack ice	98
S3	SIPEX	Pack ice, rafted sea ice	49
S4	SIPEX	Pack ice	55
S5	SIPEX	Fast ice between grounded icebergs	85
S6	SIPEX	Heavily rafted ice floes	81
S7	SIPEX	Pack ice	53
S8	SIPEX	Large level floe	37
S9	SIPEX	Heavily rafted and deformed ice	98
S10	SIPEX	Large level floe,coring site on an adjecent rafted area, probably an old chunk catched by new ice	133
S11	SIPEX	Rafted floe, ice surface very rough probably crushed together pancakes at an earlier stage	101
S12	SIPEX	Rafted ice floes	109
S13	SIPEX	Rafted floes, ice surface very rough probably consisting of thin rafted ice chunks	78
S14	SIPEX	Pack ice	64
D1	DDU	Young (approx. 3 month) fast ice, 10 cm sections	65
D2	DDU	Young (approx. 3 month) fast ice, 10 cm sections	65
D3	DDU	Young (approx. 3 month) fast ice, 10 cm sections	60
D4	DDU	Young (approx. 3 month) fast ice, 10 cm sections	60
D5	DDU	Young (approx. 3 month) fast ice, 10 cm sections	60
D6	DDU	Young (approx. 3 month) fast ice, 10 cm sections	60
D7	DDU	Young (approx. 3 month) fast ice, 2 cm sections	10
D8	DDU	Young (approx. 3 month) fast ice, 2 cm sections, snow on top	16
D9	DDU	Young (approx. 3 month) fast ice, 2 cm sections	14
D10	DDU	Fast ice (age = 1 yr), 2 cm sections	16
D-SH1 to D-SH6	DDU	Ice from sackholes in fast ice	30
D-SP1 to DSP25	DDU	Top 10 cm of fast ice	10

Table 2. Nutrient data normalized to $S = 35$, values in µmol, ikaite in mg l^{-1} melted sea ice, D-SH1 to D-SH7 from land fast ice off Terre Adélie (DDU) in November 2007, S1 to S14 from sea ice in East Antarctic (see map) between September and October 2007.

Sample	$[PO_4^{2-}]_{35}$	$[Si]_{35}$	$[NO_2]_{35}$	$[NO_2]+[NO_3^-]_{35}$	$[SNH_4]_{35}$	DON_{35}	DOC_{35}	Ikaite	TA_{35}
D-SH 1	0.50	50.30	0.12	16.17	0.37	4.91	85.99	1.03	2573.79
D-SH 2	1.53	41.39	0.14	10.63	2.04	17.50	146.17	0.68	2236.36
D-SH 3	0.30	62.18	0.05	3.06	0.45	8.45	78.80	0.22	2370.92
D-SH 4	1.33	53.12	0.07	3.11	0.91	33.41	180.04	1.23	2311.20
D-SH 5	1.77	68.80	0.11	4.71	1.47	27.75	183.44	1.58	2171.08
D-SH 6	0.45	49.83	0.08	0.98	0.32	12.51	130.84	0.53	2394.29
D-SH 7	0.47	55.53	0.03	0.20	0.77	27.59	195.34	N/A	2215.04
S1	1.75	36.37	0.14	28.48	N/A	2.40	41.52	0.34	N/A
S2	0.92	52.21	0.36	32.07	N/A	2.35	68.24	9.69	N/A
S3	1.17	40.07	0.25	28.15	N/A	4.06	49.46	N/A	N/A
S4	N/A	N/A	N/A	N/A	N/A	N/A	N/A	N/A	N/A
S5	0.64	45.91	0.18	28.18	N/A	1.59	55.68	5.89	N/A
S6	1.57	45.52	0.25	28.64	N/A	0.98	67.31	1.47	N/A
S7	N/A	N/A	N/A	N/A	N/A	N/A	N/A	0.28	N/A
S8	1.93	52.25	0.13	29.93	N/A	3.55	61.38	0.49	N/A
S9	N/A	N/A	N/A	N/A	N/A	N/A	N/A	0.87	N/A
S10	2.78	55.56	0.16	33.89	N/A	3.89	43.33	0.7	N/A
S11	0.07	54.95	0.04	3.15	N/A	4.90	73.15	N/A	N/A
S12	N/A	N/A	N/A	N/A	N/A	N/A	N/A	N/A	N/A
S13	1.44	42.63	0.10	23.78	N/A	4.94	73.14	N/A	N/A
S14	0.27	46.92	0.13	10.00	N/A	5.00	67.31	1.71	N/A

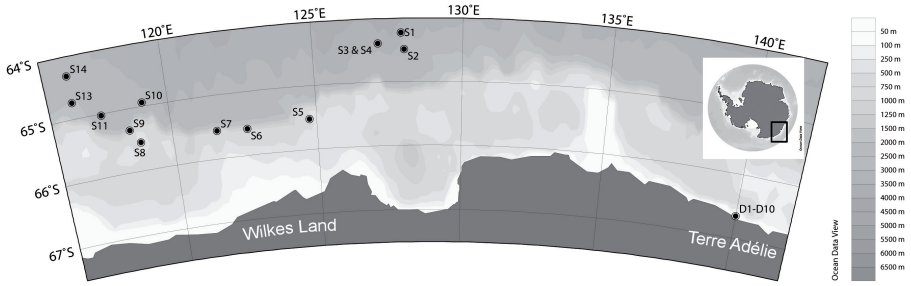

Fig. 1. Locations of ice stations sampled during SIPEX and DDU campaign.

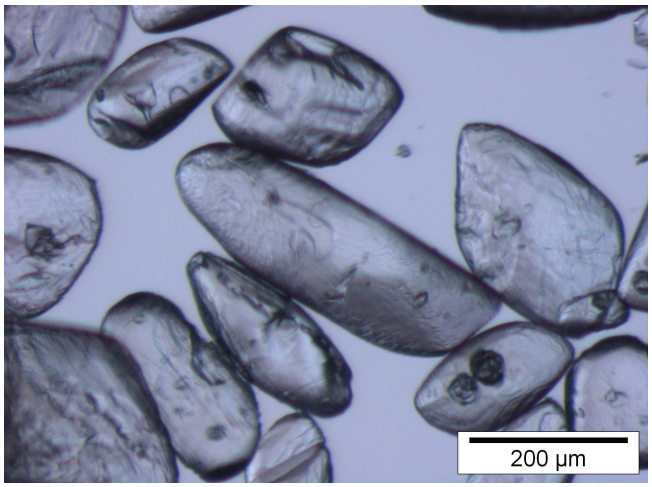

Fig. 2. Light microscopy image of ikaite crystals taken from a single bulk sea ice sample from land fast ice off Terre Adélie.

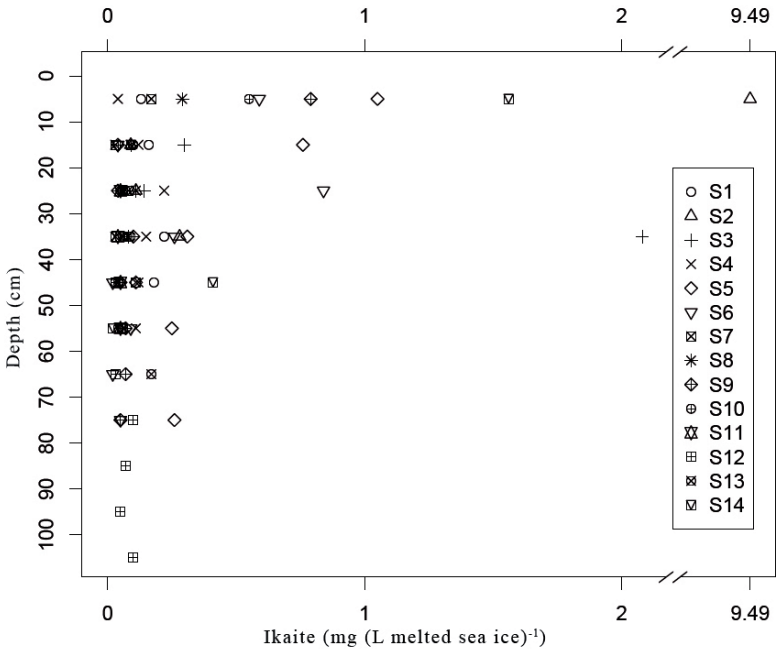

Fig. 3. Distribution of ikaite in sea ice during SIPEX cruise in different ice cores taken between September and October 2007 in East Antarctic.

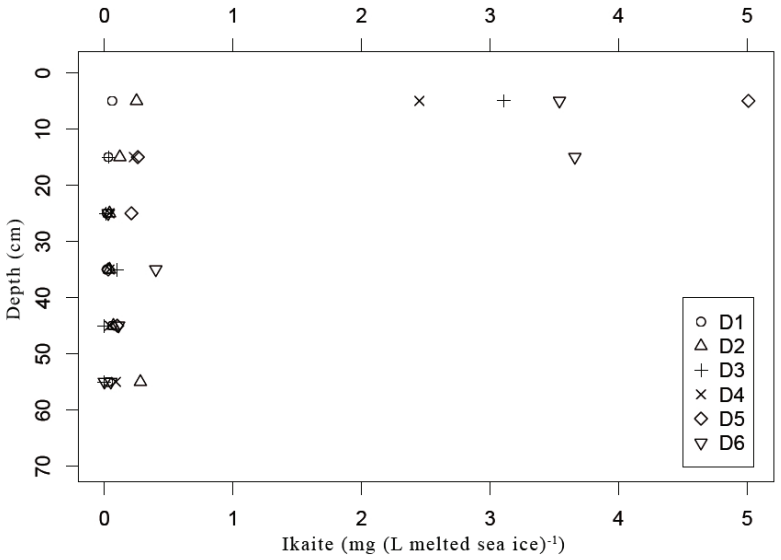

Fig. 4. Distribution of ikaite in sea ice during DDU campaign in land fast sea ice off Terre Adélie sampled in November 2007.

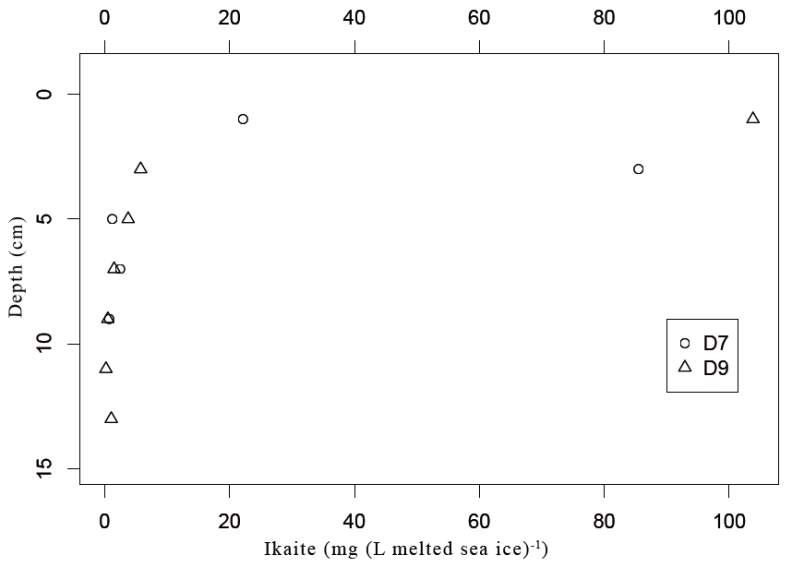

Fig. 5. Distribution of ikaite in the top layer of young (≈ 3 month) land fast sea ice off Terre Adélie (DDU).

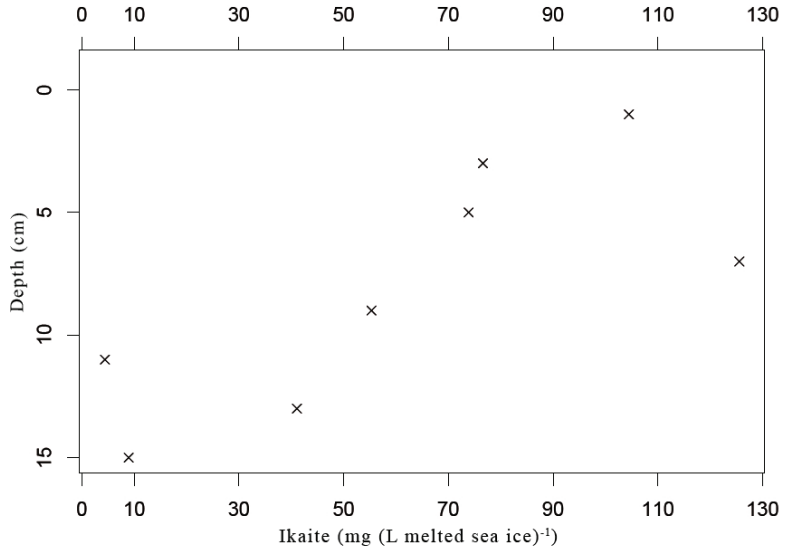

Fig. 6. Distribution of ikaite in the top layer of older (≈ 1 yr) land fast sea ice, off Terre Adélie (DDU) in November 2007 core D10.

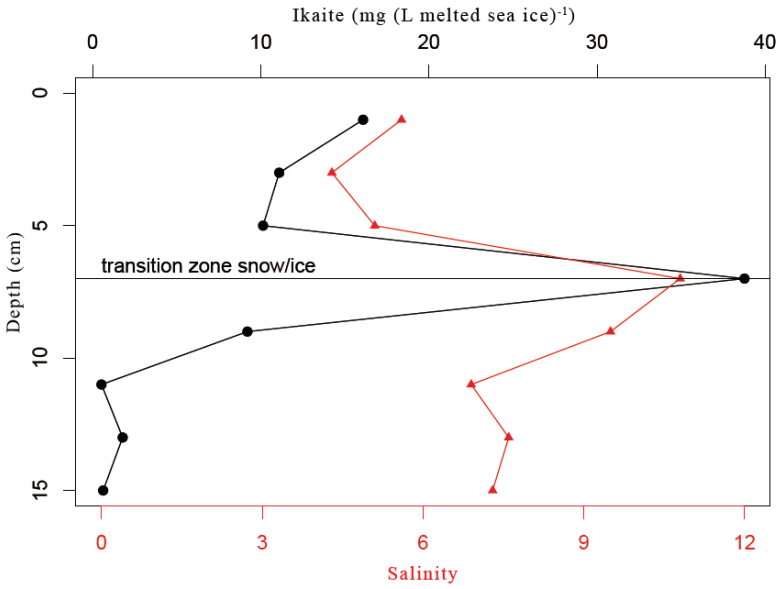

Fig. 7. Distribution of ikaite across the snow-ice interface from top layer of land fast sea ice off Terre Adélie (DDU) in November 2007, core D8, Black line = amount of ikaite, red line = bulk salinity.

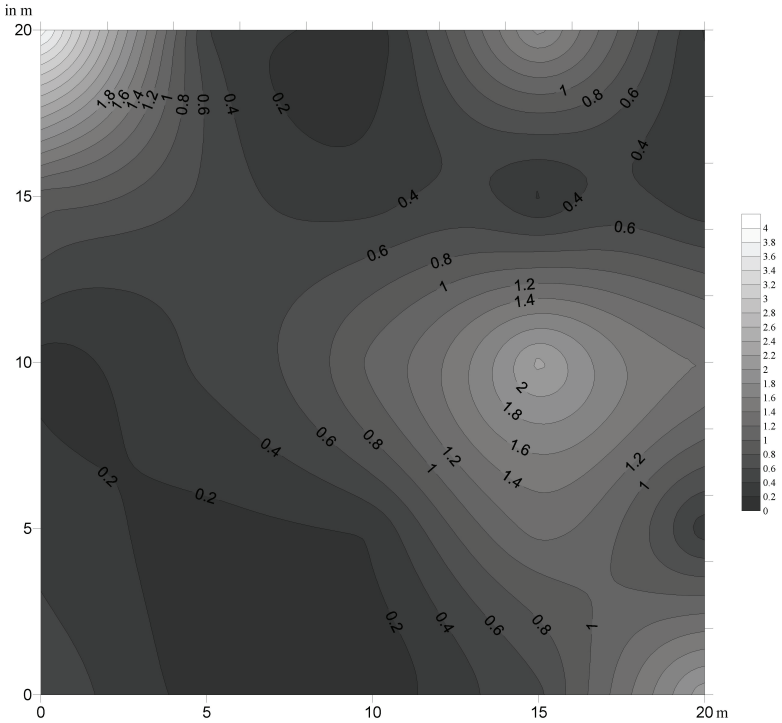

Fig. 8. Contour plot of the spatial distribution of ikaite in the first 10 cm of land fast sea ice off Terre Adélie (DDU) in November 2007 on a 20 m × 20 m grid with sample points every 5 m by 5 m. Values are in mg ikaite l^{-1} melted sea ice.